Available online at www.sciencedirect.com

SciVerse ScienceDirect

Mathematics and Computers in Simulation 98 (2014) 46–62

MATHEMATICS AND COMPUTERS IN SIMULATION

www.elsevier.com/locate/matcom

Original article

Life cycle cost, embodied energy and loss of power supply probability for the optimal design of hybrid power systems

Dhaker Abbes [a,*], André Martinez [a], Gérard Champenois [b]

[a] *Ecole d'ingénieurs en Génie des Systèmes Industriels EIGSI, 26 rue de vaux de Foletier, 17041 La Rochelle Cedex 1, France*
[b] *LIAS-ENSIP, University of Poitiers, Bat. B25, 2 rue Pierre Brousse, B.P. 633, 86022 Poitiers Cedex, France*

Received 31 December 2011; received in revised form 2 May 2013; accepted 6 May 2013
Available online 2 June 2013

Abstract

Stand-alone hybrid renewable energy systems are more reliable than one-energy source systems. However, their design is crucial. For this reason, a new methodology with the aim to design an autonomous hybrid PV-wind-battery system is proposed here. Based on a triple multi-objective optimization (MOP), this methodology combines life cycle cost (*LCC*), embodied energy (*EE*) and loss of power supply probability (*LPSP*). For a location, meteorological and load data have been collected and assessed. Then, components of the system and optimization objectives have been modelled. Finally, an optimal configuration has been carried out using a dynamic model and applying a controlled elitist genetic algorithm for multi-objective optimization. This methodology has been applied successfully for the sizing of a PV-wind-battery system to supply at least 95% of yearly total electric demand of a residential house. Results indicate that such a method, through its multitude Pareto front solutions, will help designers to take into consideration both economic and environmental aspects.

Keywords: Hybrid power system; Dynamic simulation; Multi-objective design optimization; Genetic algorithm

1. Introduction

Energy from renewable sources is being considered as a viable alternative to fossil fuels depletion. Among them, wind and solar energies have made a fast and significant breakthrough in the past 10 years. Additionally, they can be consumed locally; hence reducing both impacts from high voltage transmission lines through rural and urban landscapes, and power losses. However, neither a solar nor a wind energy standalone system can fully satisfy the load consumption due to seasonal and periodical climatic variations. Therefore, it is more reliable and efficient to install a hybrid energy system with storage due to renewable energy sources intermittent character [12]. Photovoltaic panels are often combined with wind turbines or diesel generators and batteries. To achieve such a system, finding an optimal

Abbreviations: AC, alternative current; DC, direct current; *DE*, deposition efficiency; *DOD*, depth of discharge; *EE*, embodied energy; GA, genetic algorithm; *LCC*, life cycle cost; LCE, levelized cost of energy; *LPSP*, loss of power supply probability; MOP, multi-objective optimization; PV, photovoltaic.

* Corresponding author at: Laboratory of Computer Science and Automation for Systems (Laboratoire d'Informatique et d'Automatique pour les Systèmes LIAS), National High Engineering School (ENSIP), Poitiers University, France. Tel.: +33 549453509.
E-mail addresses: dhaker.abbes@hei.fr (D. Abbes), andre.martinez@eigsi.fr (A. Martinez), gerard.champenois@univ-poitiers.fr (G. Champenois).

0378-4754/$36.00
http://dx.doi.org/10.1016/j.matcom.2013.05.004

Nomenclature

Apv (m^2) surface area of PV panels
Apv_{max} (m^2) maximum surface area of PV panels
Apv_{min} (m^2) minimum surface area of PV panels
Awt (m^2) wind turbine swept area
Awt_{max} (m^2) maximum wind turbine swept area
Awt_{min} (m^2) minimum wind turbine swept area
Cn (Ah) nominal capacity of the battery bank
$Cbat$ (Ah) nominal capacity of each battery
Cn_{max} (Ah) maximum nominal capacity of the battery bank
Cn_{min} (Ah) minimum nominal capacity of the battery bank
Cp wind turbine efficiency
Ir (W/m^2) solar radiance
$LPSP_{max}$ (%) maximum allowable $LPSP$
$Nbat$ total number of installed batteries
$Nbatp$ number of batteries strings connected in parallel
$Nbats$ number of batteries connected in series in every string
$NOCT$ (°C) normal operating photovoltaic cell temperature
Ppv (W) output electric power from the PV generator
Pwg (W) electrical power output of a wind generator
$SOCmax$ (%) maximum allowable battery storage capacity
$SOCmin$ (%) minimum allowable battery storage capacity
Ta (°C) ambient temperature
Tc (°C) photovoltaic cell temperature
$Ubus$ (V) nominal DC bus voltage
V (m/s) wind speed
$\eta acdc$ AC/DC converter efficiency
$\eta dcdc$ DC/DC converter efficiency
ηg wind turbine generator efficiency
ηgb wind turbine gearbox efficiency
ηinv DC/AC inverter efficiency
ηpc PV module power conditioning efficiency
ηpv power conversion efficiency of a PV module
ηr reference PV module efficiency
ηt wind turbine overall efficiency factor
ηwr wires losses' factor
ρ (kg/m^3) air density

configuration of the different sources considering consumer energy demand and available resources at a site proves to be essential. For this purpose, sizing and optimizing stand-alone hybrid renewable energy systems has been carried out by a number of researchers and studies [8].

Borowy and Salameh [10] for example, explicit a method to optimize the size of a PV-wind-batteries system: the desired unmet load is achieved by modifying the number of photovoltaic panels and batteries. Wind turbine, panels' type and battery technology are fixed. As there is more than one technically feasible solution, they select the less expensive one.

A procedure has been developed by Chedid and Rahman [11] that determines the optimal design of a hybrid wind-solar power system for either autonomous or grid-linked applications. The proposed analysis employs simple linear programming techniques to minimize the average production cost of electricity while meeting load requirements in a reliable way, and takes environmental factors into consideration both in the design and operation phases. Nevertheless,

components manufacture is not discussed in the paper. Only environmental impacts (such as CO_2, NO_x and SO_2 emissions due to diesel generator) are assessed. An iterative optimization method for PV-wind-batteries systems has been presented in [25]. It has been used to determine the optimum generation capacity and storage needed for a stand-alone, wind, PV, and hybrid wind/PV system for an experimental site in a remote area in Montana with a typical residential load. Generation and storage units for each system are properly sized in order to meet the annual load and minimize the total annual cost to the customer. Yang et al. [41] present a method for the optimization of a hybrid PV-wind-batteries system that minimizes the levelized cost of energy (LCE). The optimization is made by changing many parameters: components' combinations, orientation of PV modules, rated power, tower height of the wind turbine and the battery bank capacity. Diaf et al. [15] have made the optimization of a hybrid PV-wind-battery system in different locations in Corsica in France. Their optimization procedure takes on consideration loss of power supply probability (*LPSP*) and levelized cost of energy (LCE). In 2007, Shi et al. [19] proposed a robust design method for an autonomous PV-wind hybrid power system that would achieve an optimum system configuration insensitive to design variable variations. It was based on a constraint multi-objective optimization problem, which is solved by a multi-objective genetic algorithm, NSGA-II.

One year later, in 2008, Dufo-López and Bernal-Agustín [16] applied, for the first time, the Strength Pareto Evolutionary Algorithm to the Multi-Objective design of PV-wind-diesel-hydrogen-battery systems, to get an optimal compromise between three objectives: cost, pollutant emissions and unmet load.

As can be observed, most of the aforementioned studies just focus on economic cost minimization. Few investigations are focusing both on minimizing the primary energy cost while tackling the reduction of the ecological impact. This paper presents a multi-objective optimization methodology for a hybrid PV-wind-battery system. It proposes a relevant approach based on minimizing, system embodied energy (*EE*: energy required by all the activities associated to a production process on MJ or kWh) in addition of its life cycle cost (*LCC* expressed on $ or €) and loss of power supply probability (*LPSP* defined on %). Embodied energy is a concept that simplifies the assessment of the environmental impact for materials and products used; so, a full Life Cycle analysis has been done here.

In addition, to simplify the procedure and make it as affordable as possible, simple but accurate models have been performed. Moreover, photovoltaic modules' installed area (m^2), wind turbine swept area (m^2) and battery bank capacity (Ah) have been considered as decision variables for design optimization. The concept is often used for solar PV generation systems but less frequent for hybrid wind-PV-batteries systems. First, meteorological and load data are collected and assessed for a residential house in order to determine load consumption. Then, the hybrid PV-wind-battery system is modelled. This phase includes: mathematical models and components life cycle analysis in terms of economic cost and embodied primary energy. Optimization programming is done in the final step. It is carried out using a dynamic model of the global system under Matlab/Simulink and optimal configuration is obtained by applying a controlled elitist genetic algorithm for multi-objective optimization (MOP).

Thus, this paper is organized as follows: in Section 2, renewable energy sources (wind and solar) data and load profiles are assessed. Section 3 describes the hybrid system models. Next, respectively in Sections 4 and 5, optimization objectives (design and evaluation criteria) and computational method are explained. Finally, results and conclusions are presented in Section 6.

2. Data collection: renewable energy sources and load consumption profile

The first step consists in collecting data. In this section, renewable energy sources have been assessed for nine years period and load consumption has been acquired by the means of a power analyzer. Data must be accurately acquired to reach a suitable sizing of the hybrid system.

2.1. Data sources

In this study, half-hourly data used come from the National Wind Technology Centre, Colorado (latitude: 39° North, longitude: 105° West, elevation: 1855 m) website [34]. Data are available with a high accuracy and periodicity can be defined by user. In a previous paper [1], we have demonstrated that it was not necessary to choose a very low sampling

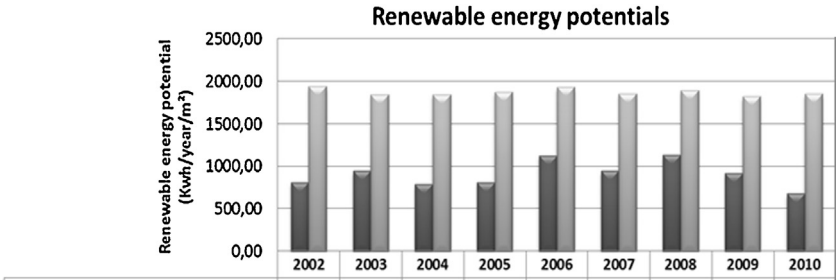

	2002	2003	2004	2005	2006	2007	2008	2009	2010
Exploitable* wind potential (KWh/year/m²)	818,38	948,21	794,15	815,67	1130,90	949,27	1135,90	919,83	683,49
Photovoltaic potential (KWh/year/ m²)	1945,72	1850,69	1851,80	1878,86	1937,10	1862,81	1898,98	1826,27	1857,48

Fig. 1. Renewable energy potentials of the National Wind Technology Center, Colorado. *Calculated using wind data speed between 3.5 m/s and 25 m/s.

period to correctly estimate produced energy. Renewable energy potentials are represented for each year in Fig. 1. They are calculated using numerical integration of the power.

$$Energy(T) = \sum_{i=1}^{8760\times 2} \frac{1}{2}(Power(i) + Power(i+1)) \times T \tag{1}$$

with T standing for the sampling interval (half an hour).

According to the graph in Fig. 1, photovoltaic potential is prevailing on wind potential for this location. Therefore, for the optimization procedure, data of the year 2010 with the lowest wind potential has been selected. The probability that design meets optimization criteria for all years, especially in terms of unmet load, has been verified by many experiments in this investigation.

2.2. Load profile

Concerning electricity energy demands, real consumption data were acquired in June for a residential home with four occupants, except cooking, heating and hot water production. The residence is occupied seven days per week all year long. All loads are supplied with 230 V AC. An half an hour acquisition period has been programmed in order to be in adequacy with renewable energy resources. Fig. 2 shows a weekday and weekend day consumption. During a

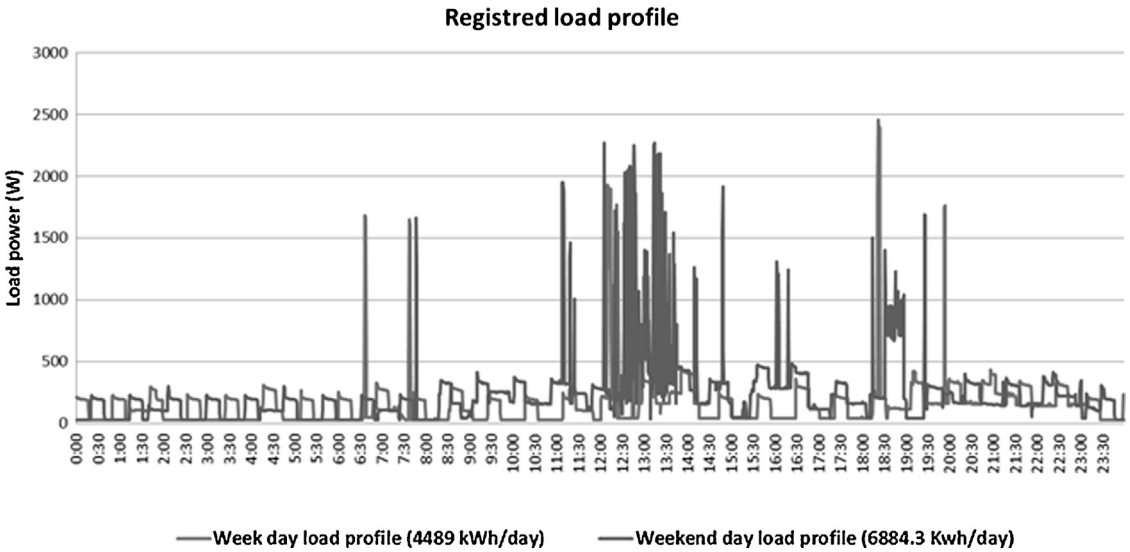

Fig. 2. Half-hourly load profile.

Table 1
Correction factors of the electric charge.

Month	Power consumption in a residential house in Poitou–Charentes (kWh)	Correction factors relative to the month of June
January	338	1.3203
February	313	1.2227
March	318	1.2422
April	248	0.9688
May	266	1.0391
June	**256**	**1.0000**
July	283	1.1055
August	287	1.1211
September	273	1.0664
October	303	1.1836
November	316	1.2344
December	338	1.3203

week day, home is less occupied by residents. The consumption has been registered at 4489 Wh/day. During a weekend day, electricity demands increase due to full occupation during the day by the family. The daily consumption then reaches 6884 Wh/day.

These profiles have been extrapolated for full year between 2002 and 2010 considering seasonal variations of the electric charge. This extrapolation has been carried out for each profile considering correction factors in Table 1. These ones were obtained through seasonal variations of the electric charge stored in a similar residential home in the region in 2009. Thereby, annual consumption of the residence is estimated at 2193 kWh/year in 2010 by using numerical integration of the power according to formula (1).

3. Hybrid system models

Modelling is an essential step before starting any phase of optimal sizing. Hybrid energy system is implemented as a combination of three power sources: wind turbine, photovoltaic generator and batteries storage as shown in Fig. 3.

A methodology for modelling each component is described below.

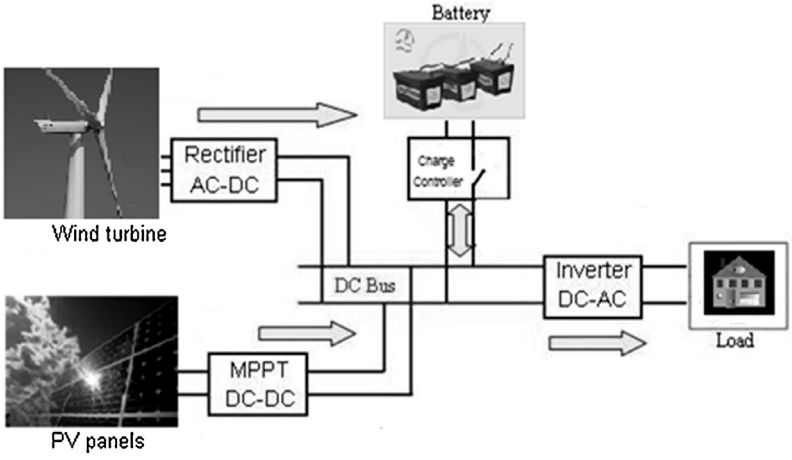

Fig. 3. Schematic diagram of wind-PV hybrid system with battery storage.

3.1. Wind turbine model

Since most home-sized wind turbines tend to operate towards the same efficiency level, rotor diameter or swept area rather than generator size makes far better criteria in order to compare various models from different manufacturers. For this reason, swept area (*Awt*) has been chosen as decision variable for wind turbine sizing. Consequently, electrical power output of a wind generator is given as follows [37]:

$$Pwg = Cp \times \eta gb \times \eta g \times \frac{1}{2} \times \rho \times Awt \times V^3 = \eta t \times \frac{1}{2} \times \rho \times Awt \times V^3 \tag{2}$$

with ρ (kg/m^3) = Air density = (354.049/*Ta*) exp(−0.034 × *Z*/*Ta*) and $\eta t = Cp \times \eta gb \times \eta g$.

All parameters are described below: *Z* (m) is the elevation and *Ta* (°C), temperature; *V* (m/s) is the wind speed; *Awt* (m^2) is the wind turbine swept area; *Cp* is the turbine efficiency; ηgb is the gearbox efficiency; ηg is the generator efficiency.

As most wind turbines available today are three-bladed horizontal axis, this technology is considered for our study with an overall efficiency factor ηt = 30% [39].

3.2. Photovoltaic generator model

Output electric power from the photovoltaic generator is given by the following equation [21]:

$$Ppv = \eta pv \times Apv \times Ir \tag{3}$$

where ηpv is the power conversion efficiency of the module (power output from system divided by power input from sun); *Apv* (m^2) is the surface area of PV panels; *Ir* (W/m^2) is the solar radiance. PV generator efficiency is given by [30]:

$$\eta pv = \eta r \times \eta pc \times [1 - \beta \times (Tc - NOCT)] \tag{4}$$

with ηr is the reference module efficiency; it depends on cell material.

For this study, a polycrystalline silicon technology has been used with 13% of efficiency [24].

ηpc is the power conditioning efficiency. ηpc is equal to 0.9 with a perfect maximum point tracker [33]. β is the generator efficiency temperature coefficient, ranging from 0.004 to 0.006 per °C. *Tc* is the cell temperature (°C). For a PV module of polycrystalline silicon solar cells, it can be estimated from the ambient temperature *Ta* (°C) and the solar irradiation *Ir* (W/m^2) as follows [29]:

$$Tc = 30 + 0.0175 \times (Ir - 300) + 1.14 \times (Ta - 25) \tag{5}$$

NOCT is the normal operating cell temperature (°C) when cells operate under standard operating conditions: irradiance of 800 W/m^2, 20 °C ambient temperature, average wind speed of 1 m/s, module in an electrically open circuit state, wind oriented parallel to array's plane, and all sides of the array fully exposed to wind. After consultation of several different polycrystalline silicon manufacturers (such as Evergreen ES-A210 or Trina Solar TSM-PA05), a typical value of *NOCT* equal to 45 °C and a typical value of β approximated to 0.0045 per °C has been considered.

For sizing optimization procedure, effective area of photovoltaic generator (*Apv*) is defined as decision variable: if *Apv* is measured in m^2, *Ppv* is numerically equal to peak power rating of the array.

3.3. Battery storage model

Many used batteries are lead-acid type in hybrid systems for a number of reasons. Discharge and recharge cycles do not significantly affect energy storage capacity. It also offers safety margin over a wet acid battery, since acid is contained in a gel and cannot be easily spilled [17]. A simple but sufficient model has been implemented for optimization method. An ideal battery model is depicted in Fig. 4. Influence of temperature on batteries capacity is not considered in this paper as we are focussing in the methodology and the model is more simple as well. However, an oversizing coefficient could be introduced when selecting batteries to consider those effects: (low temperatures reduce batteries' capacity and consequently may increase *LPSP* whereas high temperature have an impact in batteries' lifespan).

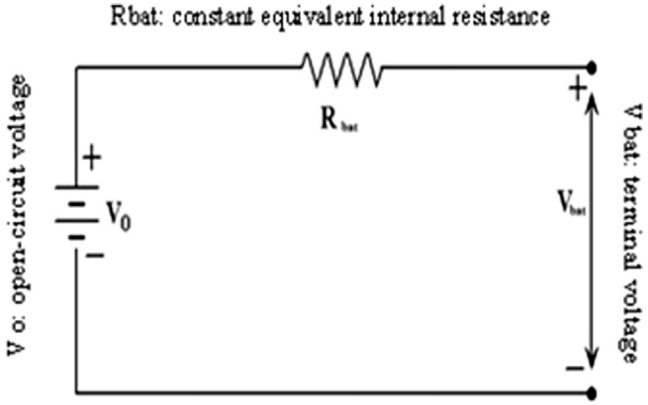

Fig. 4. Ideal lead-acid battery model.

Charging or discharging phases are controlled considering the difference between resources production (*Pres*) and load consumption (*Pload*). In charging phase, state of charge (*SOC*) can be calculated as:

$$SOC(t) = SOC(t - \Delta t) + \left(Ppv(t) \times \eta dcdc + Pwg(t) \times \eta acdc - \frac{Pload(t)}{\eta wr \times \eta inv} \right) \times \frac{\eta cha}{Ubus} \times \Delta t \quad (6)$$

In the discharging phase, *SOC* is given by:

$$SOC(t) = SOC(t - \Delta t) + \left(Ppv(t) \times \eta dcdc + Pwg(t) \times \eta acdc - \frac{Pload(t)}{\eta wr \times \eta inv} \right) \times \frac{1}{\eta dis \times Ubus} \times \Delta t \quad (7)$$

Pload(t) is the power consumed by the load at t time. Δt is the simulation time step (Δt = half an hour). $\eta dcdc$, $\eta acdc$ and ηinv are respectively DC/DC, AC/DC and DC/AC converter efficiencies ($\eta dcdc = \eta acdc = \eta inv = 0.95$ have been assumed in the literature [10,33]). ηcha and ηdis are battery efficiencies during charging and discharging phase ($\eta cha = 0.85$, $\eta dis = 1$ [22]). ηwr is introduced to consider wire losses ($\eta wr = 0.98$ [22]) and *Ubus* is the nominal DC bus voltage (48 V).

For longevity consideration, state of charge (*SOC*) is delimited by the following constraints:

$$SOCmin \leq SOC(t) \leqslant SOCmax \quad (8)$$

where *SOCmax* and *SOCmin* are maximum and minimum allowable storage capacities.

SOCmax corresponds to the nominal capacity of the battery bank, *Cn* [28]:

$$Cn = \left(\frac{Nbat}{Nbats} \right) \times Cbat = Nbatp \times Cbat \quad (9)$$

where *Nbat* = total number of batteries; *Nbats* = number of batteries connected in series in every string; *Nbatp* = number of batteries strings connected in parallel; *Cbat* (Ah) = nominal capacity of each battery; *SOCmin* corresponds to the lower limit that battery bank should not exceed when discharging. It is determined by the maximum allowable battery depth of discharge (*DOD*) as follows:

$$SOCmin = (1 - DOD) \times SOCmax \quad (10)$$

The maximum allowable depth of discharge depends on battery type and load profile. 70% depth of discharge could be tolerated [26,31].

Batteries are connected in series to reach the DC bus nominal voltage (48 V) or in parallel to obtain the desired storage capacity.

Eq. (11) calculates the number of batteries to be connected in series using the DC bus nominal voltage *Ubus* and the nominal voltage of each individual battery *Vbat*:

$$Nbats = \frac{Ubus}{Vbat} \quad (11)$$

An intelligent switcher manages batteries connection, according to four phases:

- when the charge state of batteries is below *SOCmax* (100% *Cn*) and $Pload < Pres$, the excess of energy $[(Pres - Pload) \cdot \Delta T]$ is stored in batteries. ΔT corresponds to the period of this excess state.
- when it is above *SOCmin* (30% *Cn*) and $Pload > Pres$, energy previously stored is used to support lack of energy $[(Pload - Pres) \cdot \Delta T]$ (battery discharge).
- when the state of charge is equal to *SOCmax* (100% *Cn*) and $Pload < Pres$, energy is lost $[(Pres - Pload) \cdot \Delta T]$ during the corresponding period ΔT.
- when the state of charge is equal to *SOCmin* (30% *Cn*) and $Pload > Pres$, an unmet load occurs. In this case, *Pload* must be equal to *Pres* by load shedding.

In this study, the design variable that needs optimization is total storage capacity of battery bank *Cn* (Ah): it is proportional to the number of batteries in parallel *Nbatp*. The number of batteries to be connected in series *Nbats* is not subject to optimization but is a straightforward calculation.

4. Objectives: design and evaluation criteria

Since the objective is to satisfy energy requirements from the load with a lower system life cycle cost (*LCC*) and a reduced environmental impact in terms of embodied energy (*EE*), our study will consist in finding the best configuration for the hybrid system, i.e. photovoltaic array area (*Apv*), wind turbine swept area (*Awt*) and battery bank nominal storage capacity (*Cn*). Therefore, system reliability model, components cost and primary energy analyses are studied in the following subsections.

4.1. Reliability requirements: minimizing loss of power supply probability (LPSP)

Due to intermittence of renewable energy sources, power system reliability is considered as an important step in hybrid system design process. Throughout, the reliability of the system has been expressed in terms of *LPSP* [2,9]. *LPSP* is the probability that state of charge (SOC) of batteries at any time *t*, is less than or equal to minimum value *SOCmin* and power produced by renewable sources *Pres* is less than *Pdemand* required by the load, while considering losses in the system:

$$LPSP : Pr\left\{Pres \leqq Pdemand \text{ and } SOC(t) \leqq SOCmin\right\}$$

The mathematical expression of *LPSP* corresponds to the ratio of all energy deficits to the total load demand during Δt considered period. It can be defined as [22]:

$$LPSP(\Delta t, Apv, Awt, Cn) = \frac{\sum_{t=1}^{T} DE(t, Apv, Awt, Cn) \times \Delta t}{\sum_{t=1}^{T} Pload(t) \times \Delta t} \tag{12}$$

where $DE(t, Apv, Awt, Cn)$ corresponds to energy deficit at *t* hour. It is considered when total energy available within a time interval $[(t - \Delta t), t]$ and energy stored in batteries at the beginning of this interval are insufficient to satisfy the load demand during that time period.

One of the objectives of the optimization procedure is to discover combinations between elements that give a *LPSP* lower than the maximum allowed by the user.

4.2. Cost considerations: minimizing system life cycle cost (LCC)

A second optimization objective consists in minimizing total life cycle cost (*LCC*) of the system: cumulative cost (in $ or €) throughout its life cycle, from design to recycling. In our case, the economic model of the life cycle cost includes equipment cost (*Co*), installation cost (*Cinst*), replacement (*PWreplace*) and maintenance (*PWmaint*). It is calculated knowing present worth for all components. This one is calculated as follows [33]:

$$PW = Pr \times Co \tag{13}$$

where Co is component cost and Pr represents present worth factor for an item that will be purchased n years later, and is given by:

$$Pr = \left(\frac{1+i}{1+d}\right)^n = x^n \tag{14}$$

where i represents inflation rate and d corresponds to discount rate. The life cycle cost is then given by:

$$LCC = Co + Cinst + PWmaint + PWreplace \tag{15}$$

with $Cinst$ for installation cost; $PWmaint$ for present worth of maintenance cost ($Cmaint$) and is calculated using cumulative present worth factor as follows:

$$PWmaint = (Cmaint) \times x \times x \times \frac{1-x^n}{1-x} \tag{16}$$

$PWreplace$ is present worth of the component taking in consideration the fact that it needs to be replaced periodically. In our case, we assume that price of the turbine relative to the area swept by its rotor is a good indicator. This consideration is helpful because it is indifferent to power rating or size of wind turbine's generator. Considering different Refs. [35,36], we have approximated LCC of wind turbines systems as a function of their swept area (Awt):

$$WT_{LCC}(€) = 1865.9 \times Awt + 84.158 \tag{17}$$

Calculations assume that total wind turbine initial cost is composed of about 55% for turbine and tower purchasing, 25% for installation, 10% for "balance-of-system (BOS)" costs such as cables, connectors, protections, etc. and 10% for the converter [23]. Recurrent costs just concern yearly maintenance and represent about 2.5% of whole initial investment cost. The converter will be replaced every 10 years.

For photovoltaic modules, we have assumed that purchasing price represents 50% of initial investment cost. The remaining 50% is divided between BOS (10%), converter (20%) and installation (20%). Moreover, yearly photovoltaic panels' maintenance represents about 1% of whole initial investment cost. The converter is replaced every 10 years. Thus, based on different PV installations with various models and according to the specialized website Wholesalesolar.com, LCC of a PV installation can be estimated as a function of its solar panels area (Apv) as follows:

$$PV_{LCC}(€) = 650 \times Apv \tag{18}$$

About batteries, we have chosen lead acid technology for cost and performance reasons, and supposed five replacements. Then, according to different batteries sale websites [40,14], we have approximated batteries' LCC as a function of their nominal capacity (Cn):

$$Bat_{LCC}(€) = 12.411 \times Cn + 69.05 \tag{19}$$

Note that all LCCs estimations are based on a discount rate of 5%, an inflation rate of 2% and a lifetime of 25 years. Interpolated models are represented in Fig. 5.

LCC analysis is worthwhile to guide the designer and to select components of the system. Its analysis and assessment are a tool for decision support.

4.3. Environmental impact considerations: minimizing system embodied energy (EE)

In our case, the hybrid system does not consume energy during its use, but involves the consumption of non renewable primary energy for components manufacturing. This energy is named embodied energy (energy required by all activities for production process, expressed in MJ or kWh). It is modelled and then used as a criterion for design and optimization, in order to reduce environmental impact.

For photovoltaic panels, we consider an intrinsic energy of 2300 MJ/m^2. It is the most recent value given by Stoppato [38] for a square meter of polycrystalline silicon solar panels. This value should be handled with caution because a wide disparity is observed in the literature about the primary life cycle energy embodied. Indeed, in [4,27,32], considering the case where the reference photovoltaic panels are not made from recycled materials, embodied energy is estimated as about 4600 MJ/m^2, which corresponds to twice the value given in [38]. This may be due to changes in production

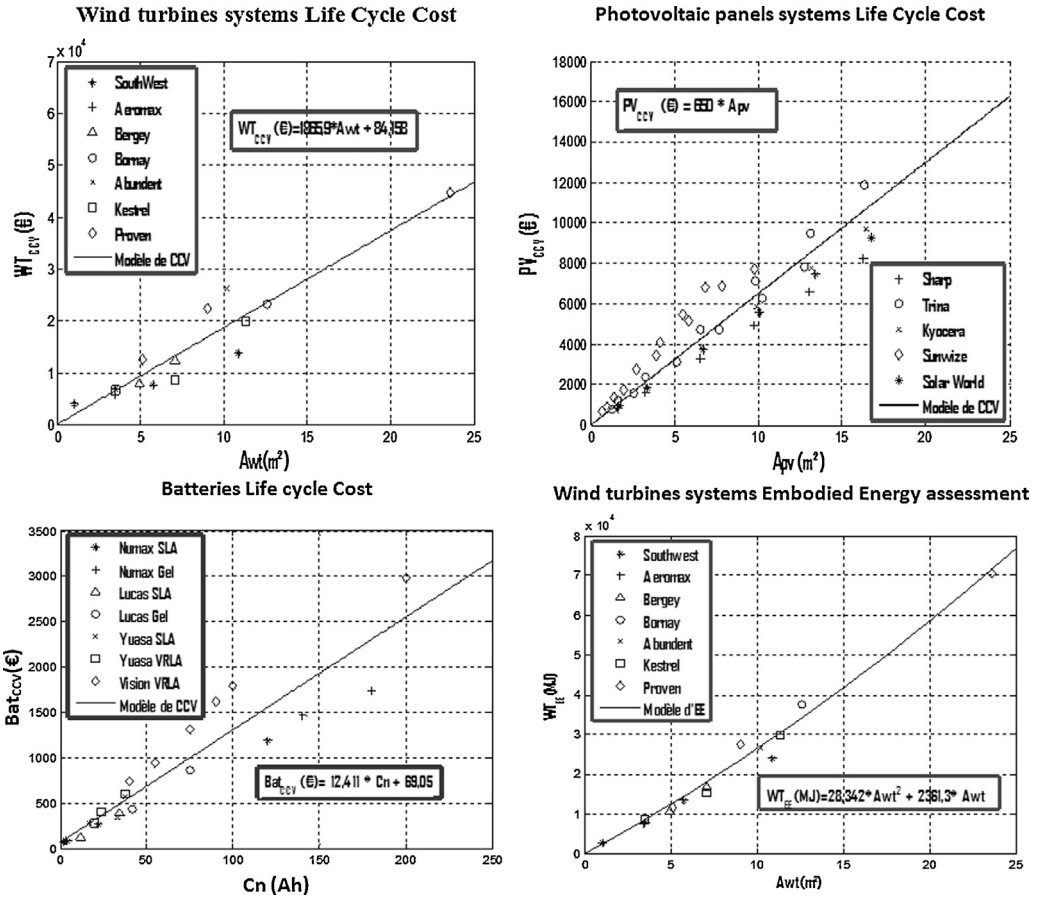

Fig. 5. *LCC* and *EE* models interpolation.

technology and wafer manufacturing processes. We must therefore keep a critical view on results, knowing that our work mainly focussed on a methodological approach and should be applied for any case.

For additional components such as cables, connectors, protection, converter and panel support, we take the data presented by Tom Markvart and Luis Castañer in their book "Practical Handbook of Photovoltaics: Fundamentals and Applications" [32]. Additional components (BOS) have primary energy needs relatively low (<10% of the installed system). We fixed the value of 300 MJ/m^2. For aluminium frame, we retain the value of 400 MJ/m^2.

For a lead-acid battery replaced five times, the primary energy was evaluated 60 MJ/Ah (for 25 years). This value assumes an optimistic recycling rate of 90% for battery metals [32] and an annual improvement of 1% in the treatment of materials and manufacturing processes [7].

Table 2 summarizes various assumptions and data used for the evaluation of embodied energy in PV systems and batteries. According to them, both primary energy embodied in photovoltaic panels (PV_{EE}) depending on their surface (Apv) and in batteries (Bat_{EE}) depending on their storage capacity (Cn) may be expressed respectively by the following linear models:

$$PV_{EE}\,(\mathrm{MJ}) = 3379 \times Apv \tag{20}$$

$$Bat_{EE}\,(\mathrm{MJ}) = 60 \times Cn \tag{21}$$

For wind turbines, data are not available in the literature, particularly for small ones; for this reason, we have conducted our own analysis. Table 2 lists assumptions and data used for small wind turbines embodied energy assessment. Information is drawn from a few references: a fact sheet prepared for the Office of Industrial Technologies, US Department of Energy by Princeton Energy Resources International, LLC [5], a study conducted by Brian Fleck and Marc Huot [18], and an example of 2 MW land-based turbine life cycle assessment presented in the book "Materials

Table 2
Assumptions and data used for energy requirements assessment for a typical installed multicrystalline silicon module and batteries.

Assumptions

(1) Data concerns a typical multicrystalline silicon PV module with aluminium frame.
(2) We assume an optimistic 90% recycling rate for scrap batteries.
(3) BOS components like cables and charge controllers contribute relatively little to the energy requirement of a solar home system (<10%).
(4) We assume an annual efficiency improvement of 1% for materials processing and manufacturing. Thus, the primary energy embodied in the batteries decrease for a replacement to another.

Data

PV module

Process	Energy requirements (MJ/m^2 module)	Energy requirements (kWh[a]/m^2)
Frameless PV module	2300	639.4
Installation of aluminium frame	400	111.2
Total module with frame	2700	750.6
Additional components (BOS)	300	83.4
Total module (installed)	3000	834

Converter

State	Energy requirements (MJ/W power)	Energy requirements (kWh/W power)
Converter (initial)	1	0.278
Converter (after 10 years)	0.9	0.250
Converter (after 20 years)	0.82	0.228
Total converter	2.72	0.756

Batteries

State	Energy requirements (MJ/Ah storage)	Energy requirements (kWh/Ah storage)
Battery (initial)	11	3.058
Battery (after 4.2 years)	10.545	2.932
Battery (after 8.4 years)	10.109	2.810
Battery (after 12.6 years)	9.692	2.694
Battery (after 16.8 years)	9.291	2.583
Battery (after 16.8 years)	8.907	2.476
Total battery[b]	60	17

[a] 1 kWh=3.6 MJ or 1 MJ = 0.278 kWh.
[b] Round number.

and the environment: Eco-Informed material choice" [6]. Some approximations are based on scaling data according weight and power.

Finally, the amount of net energy in different small wind turbines has been determined. Calculations are based on intrinsic energy of each material [20] and energy necessary in the manufacturing process. Results are presented in Table 3. According to them, wind turbines embodied energy model represented in Fig. 5 is an appropriate assessment of energy requirements for small wind turbines. The model is represented by the following expression:

$$WT_{EE}\,(\mathrm{MJ}) = 28.342 \times Awt^2 + 2361.3 \times Awt \tag{22}$$

Thus, another objective of the optimization procedure is to minimize the primary energy cost in terms of embodied energy (*EE*) as a function of PV size (*Apv*), wind turbine rotor swept area (*Awt*) and battery capacity (*Cn*).

Table 3
Assumptions and data used for energy requirements assessment for small wind turbine.

Assumptions
(1) Rotor blades are either glass reinforced plastic, wood-epoxy or injection molded plastic with carbon fibers. For calculations' standardization, we have considered molded fiber glass as we know its embodied energy.
(2) Due to lack of data, an assumption was made to include the permanent magnets in the category of aluminium because of its high embodied energy.
(3) We assume a 1% annual improvement in the treatment of materials and manufacturing processes. Thus, the primary energy embodied in the converter decreases for a replacement to another.

Component	Turbine	
	% by turbine weight	Materials' repartition
Wind turbine component weight		
Rotor		
Hub	4%	95% steel, 5% aluminium
Blades (1)	10%	100% molded fiber glass
Nacelle		
Gearbox	6%	100% steel
Generator	15%	25% magnets, 40% steel and 35% copper
Others		
Frame, machinery and shell	35%	30% aluminium, 12% copper and 5% glass reinforced plastic, 53% steel
Cables, internal supports, electronic components	30%	80% steel, 20% copper
Tower		
Tower	30 kg/m^2 swept area[a]	98% steel, 2% aluminium
Foundations		
Pile and platform	65 kg/m^2 swept area[a]	97% concrete, 3% steel

Material	Embodied energy (MJ/kg)	Embodied energy (kWh/kg)
Materials' embodied energy [20]		
Steel	24.4	6.783
Aluminium and magnets (2)	155	43.09
Copper	48	13.344
Molded fiber glass	28	7.784
Glass reinforced plastic	100	27.8
Concrete[b]	0.9	0.25
Required energy for wind turbine manufacturing		
Manufacturing process	100 MJ/m^2 swept area[a]	27.8 kWh/m^2 swept area
Primary energy contained in the other components of the wind turbine system		
BOS [estimated value]	250 MJ/m^2	69,5 kWh/m^2
Converter (initial acquisition) [4]	1 MJ/W	0.278 kWh/W
Converter (after 10 years) (3)	0,904 MJ/W	0,251 kWh/W
Converter (after 20 years) (3)	0,818 MJ/W	0,227 kWh/W

[a] Approximation based on scaling data according to weight and power.
[b] Concrete type RC30 adequate for foundations (25% cement replacement flyash).

5. Optimization procedure

5.1. Optimization problem formulation

Hybrid system optimization problem is a multi-objective design, trying to find the best compromise between life cycle cost (*LCC*), embodied energy (*EE*) and loss of power supply probability (*LPSP*). It is presented by the following mathematical formulation:

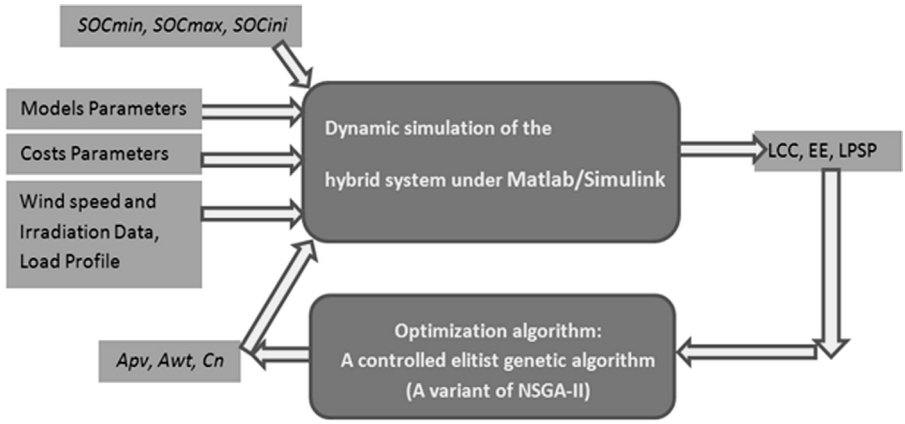

Fig. 6. Principe of design optimization programme.

Object functions: Minimum -> Hybrid system life cycle cost (*LCC*)

$$LCC(Apv, Awt, Cn) = WT_{LCC}(Awt) + PV_{LCC}(Apv) + Bat_{LCC}(Cn) \tag{23}$$

Minimum -> Hybrid system primary embodied energy cost (*EE*)

$$EE(Apv, Awt, Cn) = WT_{EE}(Awt) + PV_{EE}(Apv) + Bat_{EE}(Cn) \tag{24}$$

$$\text{Minimum} -> LPSP(\Delta t, Apv, Awt, Cn) \tag{25}$$

Constraints: feasibility for an autonomous residence:

$$Apv_{min} \leq Apv \leq Apv_{max} \tag{26}$$

$$Awt_{min} \leq Awt \leq Awt_{max} \tag{27}$$

$$Cn_{min} \leq Cn \leq Cn_{max} \tag{28}$$

where *Apv*, *Awt*, and *Cn* are the decision variables. Apv_{min}, $Apv_{\max}$, Awt_{min}, $Awt_{\max}$, Cn_{min} and Cn_{max} are lower and upper decision variables bounds specified by the user.

5.2. Computational method and algorithm

Optimization has been done using Simulink and Matlab optimization toolboxes. Fig. 6 shows principle of optimization programming. It is an iterative procedure. It runs as follows: at current iteration ($k = 0$), we have a set of parameters (initial decision variables), dynamic simulation of the system is used to evaluate the objective functions (*LCC* [€], *EE* [MJ] and *LPSP* [%]). Meanwhile, the sensitivity analysis included in the optimization method is used to determine the direction of objectives change with respect to parameters constraints. Until the stopping criteria are not satisfied, the optimization method is applied to calculate a new set of parameters considering results of the simulation and sensitivity analysis. This set of parameters is used to define the data in the following simulation.

All mathematical models of the hybrid wind-PV-battery system have been implemented in Matlab/Simulink environment as shown in Fig. 7. Main subsystems are: wind turbine model, photovoltaic array, ideal battery bank, battery controller, energy calculator and objective functions evaluators.

A controlled elitist genetic algorithm (a variant of NSGA-II [13,3]) implemented in Matlab as "gamultiobj" command is used for optimization. This algorithm always favours individuals with better fitness value (rank) that can help to increase the diversity of the population even if they have a lower fitness value. It is important to maintain the diversity of population for convergence to an optimal Pareto front. It consists of controlling the elite members of the population as the algorithm progresses. Two options, Pareto fraction and distance function, control the elitism. Pareto fraction limits the number of individuals on the Pareto front (elite members). The distance function helps to maintain diversity by favouring individuals that are relatively far away from the front. Parameters used in our case are the following: population size: 200, crossing fraction: 0.8, mutation rate: 0.2, Pareto front fraction: 0.6 and stop criterion is: maximum

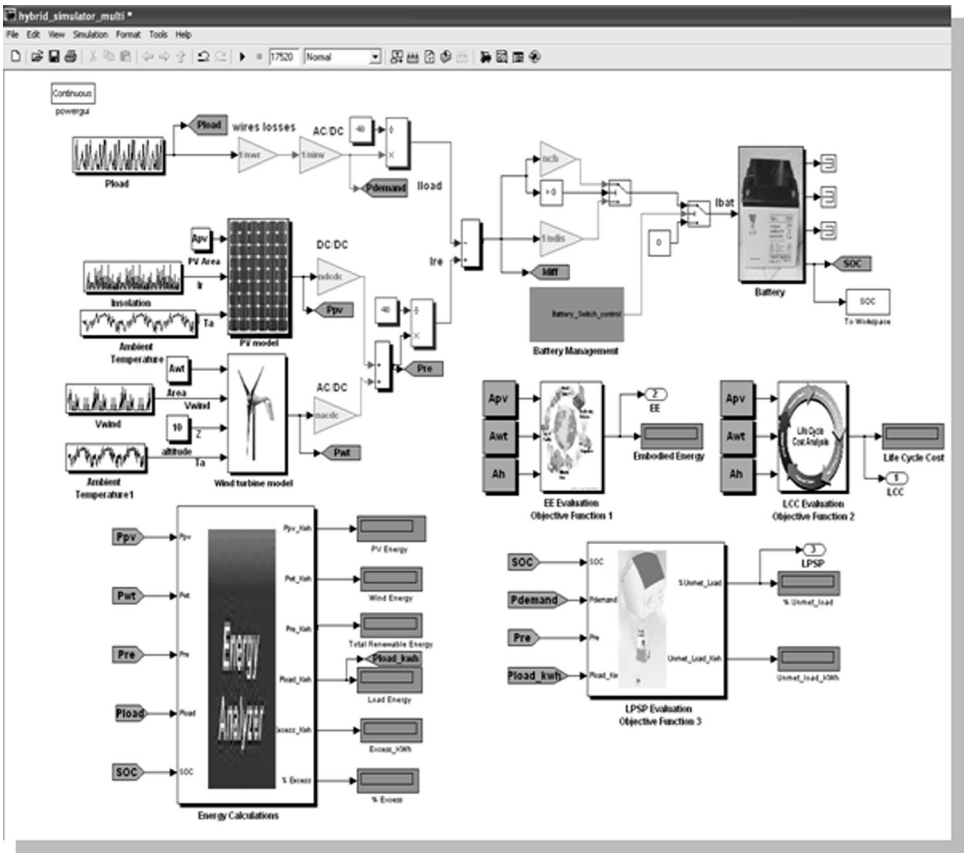

Fig. 7. Wind-PV-battery hybrid system Simulink model.

number of generation =100. Optimization routine takes a long time to compute solution, up to 5 h using an Intel Core Duo processor (CPU T6500 @2.1 GHz).

6. Results and discussion

Multi-objective optimization (MOP) seeks to minimize the three objective functions: *LPSP*, *LCC* and *EE*. Contrary to single-objective optimization, the solution of a MOP is not a single solution but a set of solutions known as a Pareto optimal set, named a Pareto border or Pareto front. Any solution of this set is optimal in the sense that no improvement can be made on one of the three objective functions without worsening at least one of them. Fig. 8(a) shows the obtained compromise surface associated with the set of "objective" functions values. A "dual-purpose" projection is made to facilitate results' interpretation. Pareto fronts obtained for all objectives are typical for a multi-objective minimization problem. Compromise surface well approximate the theoretical border. Thus, reliability of the method is proved. Fig. 8(b) presents projected optimal Pareto fronts: it shows that *LCC* and *EE* are in reality correlated. Obviously, a lesser *LPSP* implies a larger system and consequently a greater economic ("*LCC*") and also ecological ("*EE*") cost.

Fig. 8(b) shows 2D representation of the Pareto front obtained in our case. Pareto set is composed of one hundred twenty solutions. They show that, the more the consumer tolerates load shedding, the greater the hybrid system is undersized and therefore cheaper in terms of both life cycle cost and primary energy requirements. Indeed, there is a considerable variation of cost (up to 30%) between sizing a system that provides 95% and 99% of system electrical needs.

Despite the existence of multiple Pareto optimal solutions, only one of them can be chosen. In our case, the user will choose the solution that satisfies a maximum of 5% *LPSP* criterion:

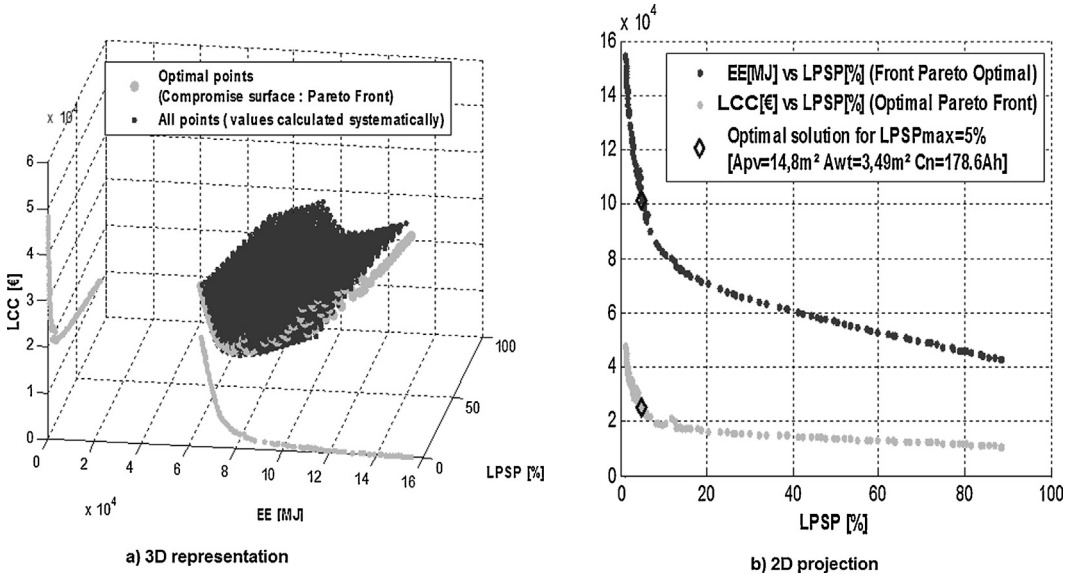

Fig. 8. Pareto front.

Table 4
Different small wind turbines embodied energy.

Product	Swept area (m^2)	Rated power of the turbine (W) (used to evaluate the energy embodied in the converter)	Wind turbine weight (kg)	Global embodied energy (MJ)	Global embodied energy (MJ)/m^2
SouthWest (Air X)	1.020	400 (at 12.5 m/s)	5.850	2663.21	2610.99
SouthWest (Whisper 100)	3.460	900 (at 12.5 m/s)	21.000	7846.49	2267.77
SouthWest (Whisper 200)	5.725	1000 (at 11.6 m/s)	70.000	13364.67	2334.44
Southwest (Skystream 3,7)	10.870	2400 (at 13 m/s)	77.000	24022.89	2210.02
Aeromax Engineering (Lacota S, SC)	3.430	900 (at 13m/s)	16.000	7565.54	2205.70
Bergey (BWC 1500)	7.070	1500 (at 12.5 m/s)	76.000	16718.42	2364.70
Bergey (BWC XL,1)	4.910	1000 (at 11 m/s)	34.000	10584.32	2155.67
Bornay (Inclin 6000)	12.570	6000 (at 12 m/s)	107.000	37431.12	2977.81
Abundant renewable Energy (ARE110)	10.180	2500 (at 11 m/s)	143.000	26630.14	2615.93
Kestrel wind (800)	3.460	800 (at 12.5 m/s)	45.000	8740.68	2526.21
Kestrel wind (1000)	7.070	1000 (at 11 m/s)	75.000	15308.68	2165.30
Kestrel wind (3000)	11.340	3000 (at 11 m/s)	150.000	29798.53	2627.74
Proven WT 0,6	5.100	600 (at 12m/s)	70.000	11485.33	2252.02
Proven WT 2,5	9.000	2500 (at 12m/s)	190.000	27422.06	3046.89
Proven WT 6	23.600	6000 (at 12m/s)	500.000	70480.75	2986.47

- Photovoltaic modules' installed area $Apv = 14.8\ m^2$ (9 Sharp ND-240QCJ 240 W panels for instance),
- Wind turbine swept area $Awt = 3.49\ m^2$, an Aeromax Engineering (Lacota S, SC) (900 W at 13 m/s) wind turbine has a close swept area of $3.43\ m^2$ with a low *LCC*,
- Battery bank storage capacity gives $Cn = 178.6$ Ah, 4 batteries Numax Gel SLG180-12,12 V/180 Ah VRLA in series can be installed.

With this hybrid system configuration (9 sharp 240 W panels, Aeromax Engineering (Lacota S, SC) Wind turbine and 4 Numax Gel SLG180-12 VRLA Batteries), we verify in Table 4, for all years, that our hybrid system provides

Table 5
Solution evaluation.

Year	Load (kWh)	PV (kWh)	Wind (kWh)	Excess (kWh)	Unmet load (kWh)	%Unmet load (*LPSP*)
2010	2193	3478	559.3	1425	88.33	4.028
2009	2198	3437	692.9	1511	82.79	3.766
2008	2205	3560	856.3	1760	57.83	2.623
2007	2198	3484	676.7	1517	64.74	2.946
2006	2198	3622	825.4	1794	48.3	2.198
2005	2196	3509	685.2	1569	75.44	3.435
2004	2198	3477	655.3	1498	71.04	3.231
2003	2201	3459	705	1546	83.92	3.812
2002	2201	3646	694.6	1689	56.4	2.562

more than 95% of the electric needs (*LPSP*< 5 %). Consequently, user does not have to incorporate another source of electricity into the system. In addition, an affordable *LCC* about 25,359 (€) [32,471$] is obtained and 101,459 MJ embodied energy is required to reach necessary energy for an entire product life cycle. *LCC* is shared and well balanced between the different components as follows: 38% for PV subsystem, 26% for wind turbine and 36% for batteries. However, total *EE* is composed of 49.3% for PV system components, 8.5% for wind turbine parts and 42.2% for batteries. This distribution is due to the fact that batteries are greedy on primary energy requirements due to their regular replacement every 4.2 years and also small wind turbines are more energy efficient than photovoltaic panels. Table 5 validates the adequacy of the proposed sizing method. For all the years, lack of production does not exceed 5% of the total yearly electric load of the hybrid residence. However, we have a considerable excess that needs somewhere to go. It can be used in cooking or in water heating supply.

7. Conclusions

In this paper, a controlled elitist genetic algorithm has been applied to the Multi-Objective design of a hybrid PV-wind-battery system for a residential house, in order to find the best compromise between three objectives: life cycle cost (*LCC*), system embodied energy (*EE*) and loss of power supply probability (*LPSP*). Optimization has been insured by a dynamic model of the system under Matlab/Simulink. Contrary to single-objective optimization, we have found a set of solutions (120) known as a Pareto optimal set. To avoid the user to add another source of energy, we have chosen a configuration that supplies the residential house with at least 95% of its electric energy requirements. It is composed of nine 240 W photovoltaic modules, one wind generator (900 W) and batteries storage of 180 Ah. Installation has a reasonable *LCC* 25,359 (€) [32,471$] and needs 101,459 MJ of embodied energy for an entire life cycle.

Triple multi-objective optimization has been achieved by the inclusion of the embodied energy as a criterion, which denotes the innovative aspect of this work among the others investigations. The analysis of primary energy requirements has been performed for each component. This analysis has provided a primary energy assessment of small wind turbines infrequently discussed in the literature due to scale overhead.

Finally, the proposed method can help designers of hybrid Wind-PV-Batteries systems to take in consideration environmental impact and not just economic evaluation. Infact, *LCC*, *EE* and *LPSP* consideration will help designers in the selection of components for the system. Their analysis and assessment are important tools for decision support.

Acknowledgement

The authors would like to thank Region Poitou–Charentes (Convention de recherche GERENER No. 08/RPC-R-003) and Conseil General Charente Maritime for their financial support.

References

[1] D. Abbes, A. Martinez, G. Champenois, J. Gaubert, R. Kadri, Estimation of Wind Turbine and Solar Photovoltaic Energy Using Variant Sampling Intervals, vol. ID 151, 2010, pp. T12-28–T12-34, 6-8 September 2010.

[2] I. Abouzahr, R. Ramakumar, Loss of power supply probability of standalone photovoltaic systems: a closed form solution approach, IEEE Transactions on Energy Conversion 6 (1) (1991) 1491–1512.
[3] J. Alonso, P. LeGresley, V. Pereyra, Aircraft design optimization, Journal of Mathematics and Computers in Simulation 79 (6) (2009) 1948–1958.
[4] E.N.E. Alsema, Energy viability of photovoltaic systems, Journal of Energy Policy 24 (14) (2000) 999–1010.
[5] D. Ancona, J. McVeigh, Wind Turbine – Materials and Manufacturing Fact Sheet, PDF Prepared for the Office of Industrial Technologies, US Department of Energy By Princeton Energy Resources International, LLC, 2001, 29 August.
[6] M.F. Ashby, Materials and the Environment: Eco-Informed Material Choice, 1st ed., Elsevier, 2009.
[7] J.D. Beet, Potential for Industrial Energy-Efficiency Improvement in the Long Term, 1st ed., Kluwer Academic Publishers, The Netherlands, 2000.
[8] J.L. Bernal-Agustín, R. Dufo-López, Simulation and optimization of stand-alone hybrid renewable energy systems, Journal of Renewable and Sustainable Energy 13 (8) (2009) 1111–1118.
[9] A. Bin, Y. Hongxing, S. Hui, L. Xianbo, Computer aided design for PV/wind hybrid system, Journal of Renewable Energy 6 (10) (2003) 1491–1512.
[10] B. Borowy, Z. Salameh, Methodology for optimally sizing the combination of a battery bank and PV array in wind/PV hybrid system, IEEE Transactions on Energy Conversion 11 (2) (1996) 367–375.
[11] R. Chedid, S. Rahman, Unit sizing and control of hybrid wind-solar power systems, IEEE Transactions on Energy Conversion 12 (1) (1997) 79–85.
[12] V. Courtecuisse, J. Sprooten, B. Robyns, M. Petit, B. Francois, J. Deuse, A methodology to design a fuzzy logic based supervision of hybrid renewable energy systems, Journal of Mathematics and Computers in Simulation 81 (2) (2010) 208–224.
[13] K. Deb, A. Pratap, S. Agrawal, T. Meyarivan, A fast and elitist multi-objective genetic algorithm: Nsga-II, IEEE Transactions on Evolutionary Computation 6 (2) (2002) 179–182.
[14] Deep Cycle Monobloc Batteries – 12 volt: http://www.tayna.co.uk, last accessed in September 2011.
[15] S. Diaf, G. Notton, M. Belhamel, M. Haddadi, A. Louche, Design and techno-economical optimization for hybrid PV/wind system under various meteorological conditions, Journal of Applied Energy 85 (10) (2008) 968–987.
[16] R. Dufo-López, J.L. Bernal-Agustín, Multi-objective design of PV-wind-diesel-hydrogen-battery systems, Journal of Renewable Energy 33 (12) (2008) 2559–2572.
[17] O. Ekren, B. Ozerdem, Hybrid Combination of Photovoltaic and Wind Energy Conversion System, Sizing and Optimization of Hybrid Energy Systems, 1st ed., Lambert Academic Publishing, 2010.
[18] B. Fleck, M. Huot, Comparative life-cycle assessment of a small wind turbine for residential off-grid use, Journal of Renewable Energy 34 (12) (2009) 2688–2696.
[19] J. hai Shi, Z. dan Zhong, X. jian Zhu, G. yi Cao, Robust design and optimization for autonomous PV-wind hybrid power systems, Journal of Zhejiang University Science A 9 (3) (2008) 401–409.
[20] G. Hammond, G. Jones, Inventory of Carbon and Energy (ICE), 2008.
[21] J. Hofierka, J. Ka nuk, Assessment of photovoltaic potential in urban areas using open-source solar radiation tools, Journal of Renewable Energy 34 (10) (2009) 2206–2214.
[22] Y. Hongxing, L. Lu, L. Burnett, Weather data and probability analysis of hybrid photovoltaic wind power generation systems in Hong Kong, Journal of Renewable Energy 28 (11) (2003) 1813–1824.
[23] T.B. Johanson, L. Burnham, Renewable Energy: Sources of Fuels and Electricity, 1st ed., Island Press, 1992.
[24] S. Kalogirou, Solar Energy Engineering Processes and Systems, 1st ed., Academic Press, 2009.
[25] W. Kellogg, M. Nehrir, G. Venkataramanan, V. Gerez, Generation unit sizing and cost analysis for stand-alone wind, photovoltaic, and hybrid wind/PV systems, IEEE Transactions on Energy Conversion 13 (1) (1998) 70–75.
[26] J.W. Kimball, B.T. Kuhn, R.S. Balog, A system design approach for unattended solar energy harvesting supply, IEEE Transactions on Power Electronics 24 (4) (2009) 952–962.
[27] C. Koroneos, N. Stylos, N. Moussiopoulos, LCA of multicrystalline silicon photovoltaic systems – Part 1. Present situation and future perspectives, International Journal of Life Cycle Assessment 11 (2) (2004), 129-136-1010.
[28] E. Koutroulis, D. Kolokotsa, A. Potirakis, K. Kalaitzakis, Methodology for optimal sizing of stand-alone photovoltaic/wind-generator systems using genetic algorithms, Journal of Solar Energy 80 (9) (2006) 1072–1088.
[29] F. Lasnier, T. Ang, Photovoltaic Engineering Handbook, 1st ed., Taylor and Francis, 1990.
[30] B. Liu, S. Duan, T. Cai, Photovoltaic dc building module based bipv system: concept and design considerations, IEEE Transactions on Power Electronics 26 (5) (2011) 1418–1429.
[31] A. Luque, S. Hegedus, Handbook of Photovoltaic Science and Engineering, 1st ed., John Wiley and Sons Ltd., 2003.
[32] T. Markvart, L. Castañer, Practical Handbook of Photovoltaic: Fundamentals and Applications, 1st ed., Elsevier, 2003.
[33] R.A. Messenger, J. Ventre, Photovoltaic Systems Engineering, 2nd ed., CRC Press, 2005.
[34] Meteorological Data Source: http://www.nrel.gov/midc/nwtc_2, last accessed in September 2011.
[35] M.R. Rivera, Small Wind/Photovoltaic Hybrid Renewable Energy System Optimization, 2008, Master's thesis.
[36] M. Sagrillo, I. Woofenden, Wind turbine buyerś guide, home power 119 (2007) 34–40.
[37] W. Shepherd, D. Shepherd, Energy Studies, 2nd ed., Imperial College Press, 2003.
[38] A. Stoppato, Life cycle assessment of photovoltaic electricity generation, Journal of Energy 33 (2) (2008) 224–232.
[39] W. Tong, Wind Power Generation and Wind Turbine Design, 1st ed., WIT Press, 2010.
[40] World's Largest Site for Batteries: http://www.atbatt.com, last accessed in September 2011.
[41] H. Yang, W. Zhou, C. Lou, Optimal design and techno-economic analysis of a hybrid solar-wind power generation system, Journal of Applied Energy 86 (2) (2009) 163–169.